Journal of Medical and Biological Engineering (2022) 42:800–815
https://doi.org/10.1007/s40846-022-00753-0

REVIEW ARTICLE

Recent Developments in Additive-Manufactured Intermetallic Compounds for Bio-Implant Applications

Po-Yuan Yeh[1] · Jacob C. Huang[2] · Jason S. C. Jang[3] · Cheng-Tang Pan[1] · Chung-Hwan Chen[4] · Che-Hsin Lin[1]

Received: 25 May 2022 / Accepted: 27 September 2022 / Published online: 21 October 2022

Abstract

Purpose This paper reviews the recent developments of two newly developed intermetallic compounds (IMCs) of metallic glasses (MGs) and high-entropy alloys (HEAs) as potential implantable biomaterials.

Methods The paper commences by summarizing the fundamental properties of recently developed MGs and high-entropy alloys (HEAs). A systematic review is presented of the recent literature about the use of AM technology in fabricating MG and HEA components for biological implant applications.

Results The high strength, low Young's modulus, and excellent corrosion resistance make these IMCs good candidates as bio-implantable materials. Recent studies have shown that additive manufacturing (AM) techniques provide an advantageous route for the preparation of glassy metallic components due to their intrinsically rapid cooling rates and ability to fabricate parts with virtually no size or complexity constraints. A practical example is conducted by AM producing a porous gradient Ti-based MG spinal cage. The produced MG powders and the in vivo test results on an 18 M-old Lanyu pig confirm the feasibility of the AM technique for producing implantable IMC-based prosthesis.

Conclusion The non-crystalline structure of MGs alloy and the random crystalline composition of HEAs provide unique material properties that will substantially impact the development of future implantable prostheses.

Keyword Intermetallic compounds · Metallic glasses · High-entropy alloys · Additive manufacturing · Implantable biomaterials

Abbreviations

AM	Additive manufacturing
BMG	Bulk metallic glass
BMGCs	Bulk metallic glasses composites
DED	Directed energy deposition
FDM	Fused deposition modeling
GFA	Glass forming ability
HMSCs	Human mesenchymal stem cells
HEAs	High-entropy alloys
HGFs	Human gingival fibroblasts
LPE	Lattice potential energy
PBS	Phosphate buffered saline
PLA	Polylactide
RHEAs	Refractory high-entropy alloys
SBF	Simulated body fluid
SLA	Stereolithography
SLM	Selective laser melting
SLS	Selective laser sintering
VEC	Valence electron concentration

✉ Che-Hsin Lin
chehsin@mail.nsysu.edu.tw

1 Department of Mechanical and Electro-Mechanical Engineering, National Sun Yat-Sen University, Kaohsiung, Taiwan

2 Department of Materials and Optoelectronic Science, National Sun Yat-sen University, Kaohsiung, Taiwan

3 Department of Mechanical Engineering, Institute of Materials Science and Engineering, National Central University, Chung-Li, Taiwan

4 Department of Orthopedics and Orthopedic Research Center, Kaohsiung Municipal Ta-Tung Hospital and Kaohsiung Medical University Hospital, Kaohsiung Medical University, Kaohsiung, Taiwan

1 Introduction

In the past decays, modern bio-implants have generally been fabricated of alloys such as SS316L, CoCrMo, Ti, or Ti6Al4V [1]. These materials have been considered good compatibility for long-term implantation. However, due to

implantation corrosion [2, 3] and low wearing resistance, the FDA has announced that hip implants carry risks including years of component material, especially, for metal-on-metal hip implants. In addition, the cobalt-chromium and the stainless alloys are prone to crevice corrosion, which may result in the release of excessive metal ions into the body [4, 5]. Moreover, the high strength of these commercial bio-implantable materials is higher than 300 GPa, which is much higher than the strength of the cortical bone of 11.5–17 GPa [6]. The high strength of the implant may cause stress shielding effects and result in another bone fracture, such alloys are usually suitable only for short-term implantation. That is, at some point, the implant must be surgically removed and replaced. Several different materials have been employed for the fabrication of bio-implants, including bio-ceramics, polymers, and new alloys. Over-developed materials, bio-ceramics have good chemical inertness, high dimensional stability, and strong bioactivity [7]. However, they are also highly brittle, which limits their practical usefulness. Polymers are beneficial for producing implantable species with low load usage since polymers have a high degree of bio-compatibility and bio-absorbability. However, their mechanical properties are far inferior to those of bio-ceramics or alloys [8].

Alternatively, intermetallic compounds are complexes composed of two or more elemental metals. IMCs differ from traditional alloys in that the metal elements exist in discrete proportions, whereas in alloys, their concentrations vary continuously. Broadly speaking, IMCs can be categorized as either metallic glasses (MGs) or high-entropy alloys (HEAs), depending on their crystalline structure, number and proportion of metallic elements, configurational entropy, and so on. Manufacturing MGs and HEAs is challenging due to their complex compositions. These new alloys have many attractive mechanical, chemical, and biological properties, and have thus attracted significant interest in many applications in recent decades. In general, intermetallic compounds have many advantages for the fabrication of biological implants, such as a low Young's modulus and a passivation layer on the surface, which improves the corrosion resistance and inhibits the release of toxic metal ions into the body. In addition, these new alloys can be produced as a bio-degradable metal that provides short-term strength and then is degraded and resolved in the tissue for long-term tissue regeneration purposes. For example, Mg-based biodegradable alloys have thus been proposed as a more feasible candidate for long-term implants [9]. Accordingly, the feasibility of utilizing MGs and HEAs for the fabrication of bio-implants has attracted growing attention in the literature. However, the delicate materials properties of these new intermetallic compounds rely on special composition design and unique fabrication processes. Thanks to the recent developed metal additive manufacturing technology, the super-fast cooling rate during laser machining makes it possible to produce delicate metal structures with amorphous microstructures. In these regards, AM techniques have been widely used to fabricate various intermetallic compounds for bio-implants applications.

This paper aims to introduce the fundamental properties and recent materials designs for the two major categories of the new intermetallic alloys of MGs and HEAs. The materials properties and the corrosion resistance behaviors of the newly designed IMCs were collected and compared. A systematic review has been conducted, pertaining to the use of AM technology in fabricating MG and HEA components for biological implants. This paper provides a quick way to learn the fundamentals and recent developments for AM-produced IMCs for biomedical applications.

2 Brief Overview for Two Major IMCs

Table 1 summarizes the mechanical and electrochemical properties of the recent developed IMCs. The yield strength, Young's modulus and the measured corrosion potential for the MG and HEA IMCs are compared with that of cortical bone and other commercially available metal prostheses. It is clear that the cortical bone has a far lower yield strength and Young's modulus than the stainless and commercial Ti6Al4V and CoCrMo alloys. Alternatively, metallic glass materials exhibit relatively low Young's modulus and high yield strength, which is beneficial for producing bone prosthesis for high loading applications. Moreover, the electrochemical corrosion potential of typical Ti-based and Zr-based MGs is much higher than that of commercial Ti alloys and stainless steel, indicating higher corrosion resistance for these MGs and lower risk of ion release into the body fluid after implantation. For potential bio-degradable Fe-based and Mg-based MGs, they provide shorter high strength and low Young's modulus for the attachment of newly grown tissues. The high reactive elements in these two MGs degraded and are then absorbed into the body after a period after implantation, leaving only the biological tissues after the degradation. It is also noted that the porous MGs have an even lower modulus near the modulus of typical cancellous bone, which provides the possibility for simultaneously constructing the cortical bone and the cancellous bone using the AM process to mimic the real bone structure.

2.1 Metallic Glass

Metallic glass, as its name suggests, is a metal alloy with glass properties. Most traditional alloys have a polycrystalline structure, wherein the grain boundaries effectively form a type of defect in the material. Takeuchi and Inoue [34] proposed the following general rules of thumb for the definition

Table 1 Mechanical and chemical properties of different IMC system, cortical bond and other commercial biocompatible metals

	Materials	Processing method	Yield strength (MPa)	Young's Modulus (GPa)	Corrosion potential (mV)	References
MG	ZrCuFeAlAg	Copper mold casting	1700 ± 28	82 ± 19	− 416 ± 7 (in SBF)	[10]
		Selective laser melting	1670 ± 36	79 ± 2	–	[11]
		Selective laser melting (70% porosity)	350 ± 10	13 ± 1	–	[11]
	ZrCuFeAl	Copper mold casting	–	50	–	[12]
	ZrCuAlAg	Copper mold casting	1910	92	− 555 ± 30 (in Hank's)	[13]
	ZrCuNiAl	Copper mold casting	1865	102	− 575 ± 20 (in Hank's)	[13]
		Selective laser melting	1504 ± 103	70	–	[11]
	ZrTiNiCuAl	Copper mold casting	1813	100	− 646 ± 40 (in Hank's)	[13]
		Selective laser melting	600–1500	85	–	[11]
	TiZrNiCuBe	Copper mold casting	1645	95	− 625 ± 40 (in Hank's)	[13]
	ZrTiAlFeCuAg	Copper mold casting	1450 ± 20	70 ± 1	− 184 ± 36 (in PBS)	[13]
	TiCuZrFeSnSiAg	Copper mold casting	2010	100.4 ± 0.1	− 110 ± 40 (in PBS)	[14]
	TiZrHfCuNiSiSn	Copper mold casting	2000 ± 78	80 ± 12	–	[15]
	TiZrCuPdSn	Copper mold casting	> 2000	93.3	–	[16]
	TiZrTaSi	Copper mold casting	–	90	− 436 ± 34 (in Hank's)	[17]
		Hot pressing (54% porosity)	144	8.6	–	[18]
	TiZrSiTaCoSn	Hot pressing (72.4% porosity)	19	2.3	–	[19]
	FeCoCrMoCBY	Copper mold casting	–	–	− 570 (in PBS)	[20]
		Selective laser melting	3.5	213	–	[21]
	FeMoPCB	–	2900	–	–	[22]
	FeCrMoPC	Copper mold casting	–	-–	− 317 ± 13 (in Hank's)	[23]
	MgZnCa	Copper mold casting	716–854	48	–	[24]
	MgZnCaSr	Copper mold casting	848 ± 21	18.9 ± 0.1	–	[25]
	MgNdZnZr	Selective laser melting (porous structure)	9.4 ± 0.65	0.466 ± 0.035	–	[26]
HEA	TiTaHfNbZr	RF sputtering on Ti64	12,150 ± 340	181.3 ± 2.4	–	[27]
		Copper mold casting	800–985	80	− 391.16 (in PBS)	
	$TiZrHfNbFe_{0.5}$	Copper mold casting	1100	50	− 300 ± 10 (in PBS)	[28]
	TiZrNbTaMo	Copper crucible casting	1356	115.49	− 900 (in PBS)	[29, 30]
		Selective laser melting	1690 ± 78	140 ± 9	–	[29]

Table 1 (continued)

	Materials	Processing method	Yield strength (MPa)	Young's Modulus (GPa)	Corrosion potential (mV)	References
Bone and others	Cortical Bone	–	130–150	10–40	–	[31]
	Cancellous Bone	–	Axial: 4.5 ± 0.9	Axial: 0.431 ± 0.217	–	[32]
			Transverse: 1.6 ± 1.0	Transverse: 0.127 ± 92		
	CoCrMo	CNC machining	450–1030	210–255	− 444 ± 135 (in PBS)	[31]
	Ti6Al4V	CNC machining	760–1050	101–125	− 435 ± 44 (in PBS)	[31]
		Selective laser melting	967–978	115	–	[11]
	316L SS	CNC machining	190–690	193–210	− 221 ± 7 (in PBS)	[31]
		Selective laser melting	430–512	193–210	–	[11]
	Pure Ti	CNC machining	170–485	102.7–104.1	–	[33]
		Selective laser melting	560 ± 5	113 ± 3	–	[11]

of amorphous alloys, including a multi-component system consisting of three or more elements, significant differences (more than 12%) among the atomic size ratios of the three main components and a negative heat of mixing between the three main components. In general, metallic glasses have a unique atomic structure, so they do not contain microstructural defects such as vacancies, dislocations, twins, or grain boundaries. In addition, metallic glasses usually have more promising corrosion-resistant properties due to their amorphous structure. The amorphous structure of metallic glass makes it a low modulus and high elastic strain limit [35, 36]. Nevertheless, metallic glass is typically composed of various atoms of different atomic sizes, such that the mechanical properties of MGs can be designed and adjusted. Figure 1 shows the basic mechanical properties of some of the most common metallic biomaterials. It is clear that the metallic glass materials exhibit a wide range of the Young's modulus and yield strength compared to that of other crystalline materials. In addition to the favorable mechanical properties described above, MGs also have good chemical properties compared to traditional alloys. Furthermore, in contrast to traditional alloys, which are mostly polycrystalline and liable to corrosion at the grain boundaries. MGs have an amorphous structure with greatly improved corrosion resistance. Not only that, but the corrosion resistance can be further enhanced through the addition of Cr, Mo, and P [37].

Metallic glass was first discovered by Klement, Willens, and Duwez in the amorphous state of an AuSi alloy [46]. Since that time, many MG systems have been developed with compositions including Pd-, Pt-, Zr-, Fe-, Ti-, Mg-, Co- and Au-based systems [47]. Traditionally, MGs have been applied mainly in the engineering field [36]. However, their potential

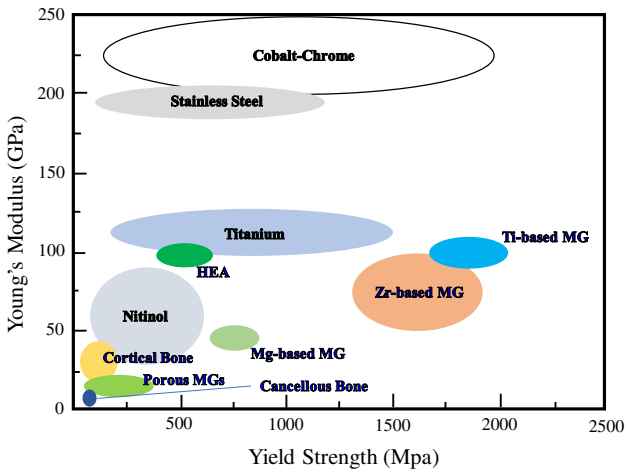

Fig. 1 Mechanical properties of cortical bond and various metal alloys used for producing implantable devices. The data for Ti-based MGs are from [14–17, 38], Zr-based MGs are from [10, 12, 13, 39], Fe-based MGs are from [21–23], Mg-based MGs are from [24, 25, 40], HEA are from [27–30, 41–43], Porous BMG are from [11, 20, 44, 45]

for application in the biomedical field has attracted growing attention over the past several decades [48]. Unlike typical crystalline alloys, MGs have an amorphous structure, like glass, and have a glass transition temperature (Tg) lower than their crystallization temperature (Tx), and between these two temperatures, they have plastic-like properties. However, the atoms conjugate and form a crystal structure at a low cooling rate below the melting temperature. Therefore, superfast cooling for forming the amorphous structure for the MG system is essential. In addition, the ease of making MGs also depends

on the glass-forming ability (GFA) of the alloy system. In particular, the lower the GFA, the higher the cooling rate must be. The critical cooling rate required for the earliest binary metallic glasses was as high as 10^7 K/s, which posed significant challenges to manufacturing. However, through the addition of other metal elements to the binary system, the critical cooling rate has now been reduced to the order of around 10^3 K/s [49, 50]. However, the metallurgy process provides the cooling rate of 10^2 K/s or even lower, which is difficult to form a metallic glass structure, especially for the bulk orthopedic implants. The cooling rates of the material surface and the inner part are different, and they may form different alloy structures from the outside to the inner parts. Alternatively, the cooling rate for selective laser melting provides a high cooling rate of 10^5 K/s during the AM manufacturing process [51]. The high cooling rate and the layer-by-layer formation of the designed structure provide the possibility for producing bulk implantable prosthesis with amorphous microstructure. Therefore, a great amount of research has been reported on producing bulk metallic glasses using selective laser melting techniques.

2.2 High-Entropy Alloy

High-entropy alloy is another category for intermetallic compounds which exhibit different material properties compared to metallic glass. Conventional alloys are typically composed of one or two metal elements in the structure, and other elements of minor ratio are added as required to achieve the desired material properties. For example, steel is based on Fe with Co and Ni added to make it less prone to rust. In contrast, in 1995, Yeh [52] introduced a new class of alloy system, referred to as high-entropy alloys (HEAs), consisting of five or more main alloying elements with high mixing entropy and a concentration of 5–35 at% each. His research opened the new field for intermetallic compounds and inspired several researchers working on this new specialty metal alloy system. Research on HEAs has grown exponentially since 2004 [53]. While early studies focused mainly on the structural application and the material property characterization of HEAs, more recent research has investigated the potential of HEAs as bio-implant materials [54]. For example, several studies have considered the use of HEAs as implant coating materials [55–59], while others have explored their feasibility for bone implant [60] and dental implant [61] applications.

For multi-component alloys, with n elements mixed at an equal atomic ratio to form a solid solution, the mixing entropy can be expressed as [62]:

$$\Delta S_{conf} = R \ln n$$

Where ΔS_{conf} is the material configuration entropy, R is the gas constant (8.314 kJ/mol), and n is the element species that compose the material. A simple inspection of the formula reveals that the mixing entropy exceeds 1.609R when the number of elements in the alloy reaches five, or more, and it is for this reason that such alloys are referred to as HEAs. In general, low entropy alloys are with the mixing entropy $\Delta S_{conf} < R$ and HEAs are with $\Delta S_{conf} > 1.5R$. Other alloys are defined as medium-entropy alloys. Due to the different characteristics of their various elements, HEAs possess many interesting properties and effects that are not observed in traditional alloys. Broadly speaking, these effects fall into four core categories, as described in the following.

2.2.1 High-Entropy Effect

In the solid state, HEAs consist of an elemental phase, random precipitation phase (random solid solution phase) and an IMC phase. The random precipitation phase is the ideal internal structure of HEAs, and it has profound effects on the properties of the alloy. For example, similar to the case of steel strengthened by the precipitation of carbon, the random precipitation phase in HEAs results in a far higher strength than that of general alloys. Moreover, the phase has a relatively high entropy value, and hence, HEAs tend not to deform or melt very quickly when heated at high temperatures. Among the various types of phase that can exist in alloy systems, the solid solution phase has the highest mixing entropy [63]. Thus, in multi-element alloys, this characteristic contributes to the formation of random solid-solution phrases rather than IMC phases. However, the factors affecting the formation of this random solid solution phase also include the mixing enthalpy [63, 64], the atomic size difference, and the valence electron concentration (VEC) [64]. In addition, when HEAs are annealed at relatively low temperatures, the random solid solution phase may transform into an intermetallic phase [65].

2.2.2 Sluggish Diffusion Effect

HEAs have a slow diffusion effect. As a result, they are less prone to structural changes such as grain growth or recrystallization, which also makes HEAs stable at high temperatures. The slow diffusion effect occurs since each vacancy in HEAs is surrounded by a different atom, resulting in a different lattice potential energy (LPE) for every vacancy. The same phenomenon also leads to the influence of diffusion kinetics within the HEAs [66]. Early studies examined the one-dimensional diffusion phenomenon in alloys using random walking models with random LPE bias [27, 67]. The results showed that LPE changes on diffusion were limited to binary systems. Thus, Tsai et al. [66] employed a quasi-binary method combined with the Sauer-Fraise method to analyze the diffusivity of a pure face-centered cubic crystal Co-Cr-Fe–Mn-Ni alloy system.

2.2.3 Severe Lattice Distortion Effect

The lattice structure of HEAs is composed of elements of various sizes, and these differences in size between them produce different stresses and strains on the nearby lattice. The resulting lattice distortion enhances the mechanical properties of HEAs [68]. However, it also prompts the scattering of electrons and phonons, and therefore reduces electrical and thermal conductivity [69, 70]. Furthermore, the twisted lattice structure also diffuses X-rays, resulting in a low diffraction peak intensity [71].

2.2.4 Cocktail Effect

The cocktail effect of HEAs was first proposed by Ranganathan [72], who showed that the final properties of HEAs are dependent on the basic features and mutual interactions of the various elements of the alloy. The high complexity of the atoms in the alloy formed various heterogeneous structures such that the cocktail effect was presented. For example, the strength and ductility of CrMnFeCoNi HEA can be further enhanced through adding Al since Al prompts a change in the internal structure from FCC to BCC [73, 74].

Therefore, HEAs can inhale more external energy by reducing the internal entropy compared to typical pure metals or medium entropy alloys. The mechanical property of HEAs is close to the cortical bone, which is beneficial for matching the materials property of nature bone structure in orthopedic prostheses. However, a low cooling rate during HEAs production provides more time for atom diffusion, which may result in the formation of uncontrollable intermetallic phases. The rapid cooling rate of the AM process limits atom diffusion such that the desired microstructure remains after the fabrication of HEAs species. Therefore, the mechanical and electrochemical properties of the HEAs produced with the AM process is more controllable.

2.3 IMCs Produced with Additive Manufacturing Technology

Additive manufacturing (AM), also called 3D printing, is highly efficient approach for fabrication of components with complex geometries, high precision, material savings, design flexibility, and customization [75]. One of the first AM methods was that of stereo-lithography (SLA) developed in 1986 [76]. However, many different AM techniques have been developed since then, including fused deposition modeling (FDM) [77], selective laser sintering (SLS) [78], selective laser melting (SLM) [79], and direct energy deposition (DED) [80]. Traditional machining removes unnecessary parts by turning, milling, etc., and processes the desired shape. This method is limited by space, making some complex geometries impossible to manufacture. Additive manufacturing, on the other hand, is formed by stacking layer by layer, so that complex geometries can be produced. Not only that, but AM technique, such as SLM, break down the cooling process into manifold steps, each of which is sufficiently fast to guarantee glass-formation [81–83]. Additive manufacturing is employed in many fields nowadays, including the aerospace industry [84–86], biomedical industry [87, 88], construction industry [89, 90], and so on.

Additive manufacturing has many benefits to produce bio-implants. For example, it is extremely versatile in terms of the size, geometry, and complexity of the parts that it can produce. Hence, it is ideally suited to the fabrication of parts customized to the requirements of particular patients. Figure 2 shows the designed porous gradient spine model and the AM-produced porous gradient spine cage for spine fixation surgery. Cortical bone and cancellous bone can be simultaneously produced in a single process. Moreover, AM techniques could fabricate porous structures and even porous gradient structures to match the Young's modulus of real bone structure [91–93]. The holes also provide the space for the bone cells to conduct osteointegration such that stress shielding phenomenon can be reduced [94, 95]. Therefore, the AM process is ideal for procuring custom-made implants with desired material properties. Figure 3 shows the process

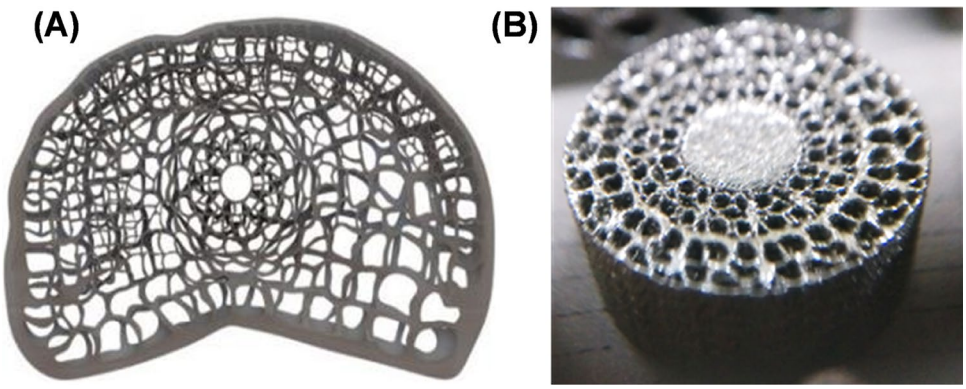

Fig. 2 **A** The designed model for porous gradient spine cage **B** An example for the AM produced porous gradient prosthesis

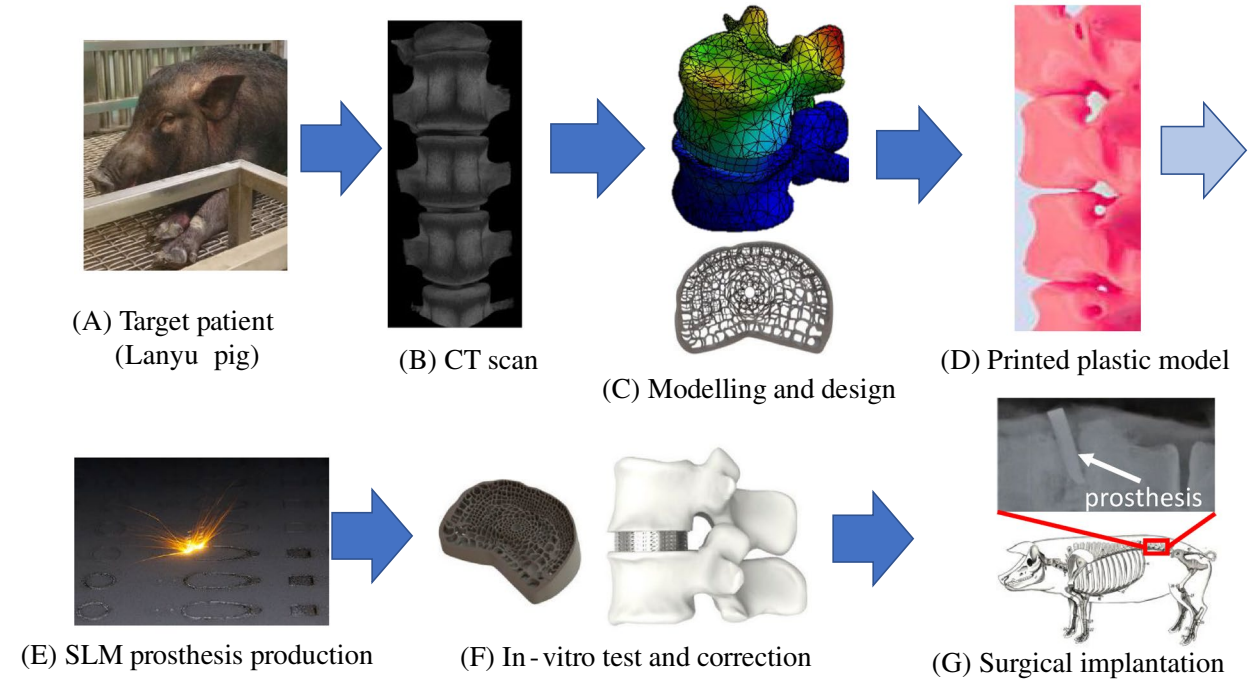

Fig. 3 Schematic showing the typical process flow for producing custom-made implant

flow for producing a custom-made implant using the metal SLM AM process. An example regarding the SLM spinal cage for animal implantation tests is used to showing the process. First, target patient, here we use Lanyu pig as the example, is scanned with high-resolution CT. The obtained images are then converted to a digital model for the prosthesis design, as shown in Fig. 3C. A plastic model is produced using 3D printing to have a real model showing the real spine structure (Fig. 3D). The designed prosthesis is then produced with the SLM process and then in-vitro test by combining the printed metal species and the plastic model (Fig. 3E and F). Finally, the produced prosthesis is then implanted into the target position with surgery operations (Fig. 3G).

3 Various 3D Printed MGs for Biomaterial Applications

The material characteristics of metallic glasses are bifacial for producing biomedical implants, especially for orthopedic applications. The mechanical and chemical properties of MGs can also be designed by mixing various metal elements of different compositions. In general, non-toxic elements such as titanium, zirconia, silicon, tantalum and even cobalt are preferred. Titanium and its alloys are the most common for producing bio-implants due to their excellent bio-compatibility and long-term clinical validation [1]. However, titanium exhibits a high melting temperature of 1,668 °C which makes the titanium alloy difficult to form metallic glass texture during fabrication. Therefore, it is essential to reduce the melting point of Ti-based alloys by introducing various elements. This is the very first important step for producing Ti-based MG powder using the powder atomization technique. Figure 4 shows the typical melting point for various Ti-based MGs. It is clear that the TiSn and TiZr MG systems have high melting temperatures of higher

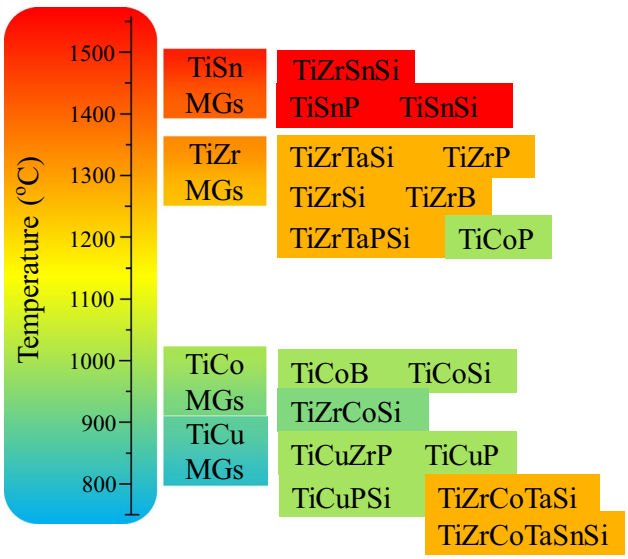

Fig. 4 Schematic showing the melting point of various Ti-based MG compositions

than 1200 °C which is difficult to be molten and atomized. In contrast, the TiCu-based MG has lower melting point which make it easy to be produced. Nevertheless, copper is considered a toxic element that is not recommended to be used for producing implantable medical devices. To lower the melting temperature of the popular TiZr alloys, more elements such as Si, Ta are added to form the MGs composed of more than 5 elements [96]. The melting temperature of these MG systems can be as low as around 800 °C. Figure 5 presents the SEM images for the produced TiZrTaSiSnCo 6-element MG powders using atomization technique and the XRD diffraction patterns for the powders of different size ranges by the authors' group. The SEM images showed that the produced powder had a perfect round shape, which is beneficial for the AM process (Fig. 5A and B). The XRD results also indicated that the produced powders of a size smaller than 63 µm were with an amorphous structure, as shown in Fig. 5C. The round shape and the amorphous structure of the atomized MG powders are essential for producing bulk amorphous prostheses using the SLM process. Below reviews the recent progress of various metallic glass systems as implantable biomaterials.

3.1 Zr-Based Metallic Glass

Zr and Ti have similar biocompatibilities and are both inert and non-toxic metals. Zirconium oxides are commonly used as dental implants due to their high mechanical strength and good corrosion resistance [97]. Furthermore, pure Zr and Zr alloys have a lower Young's modulus than Ti and its alloys, and thus effectively lower the stress shielding effect [10]. Consequently, Zr-based MGs have increased potential for the realization of biological implants. Liu et al. [12, 39] and Sun et al. [98] prepared Ni-free, Zr-based MG (ZrCuFeAl) for biomedical applications using an arc melting technique. Both materials had a high fatigue strength and fracture toughness. Moreover, with a value of around 82 ± 1.9 GPa, the Young's modulus was lower than that of pure Ti and its alloys. Sun et al. [99] performed cytotoxicity tests and in vitro corrosion tests on Ni-free and Ag-bearing Zr-based metallic glasses. The cell culture performance of the Zr-based MG was found to be superior to that of traditional Ti6Al4V alloy. The corrosion performance of the Ag-bearing Zr-based MG was also better than that of Ti6Al4V in Hank's solution. Notably, due to the presence of a surface passivation layer on the Zr-based MG, the daily average concentrations of Cu, Fe, and Al ions released in simulated body fluid (SBF) were found to be just 1.4, 7.2, and 5.6 ppb [39], respectively, and were hence far lower than the concentrations judged to be harmful to the human body [100]. Not only that, but the low concentration of released Ag ions has an antibacterial effect, which is beneficial in reducing the risk of infection following implantation [47, 101].

Hua et al. [102] prepared Ni-free Zr, TiAlFe, and CuAg bulk metallic glasses (BMGs) for biomedical applications using a copper mold process. The test results showed that the compression plasticity and notch toughness of the Zr-based MG increased with increasing Zr content. Furthermore, when tested on L929, MG63, and MC3T3-E1 cell culture solutions, the cell adhesion and proliferation activity of the Zr-based MG were similar to those of Ti6Al4V. The cytotoxicity of the Zr-based MG (0–1 grade) was also similar to that of Ti6Al4V. Sun et al. [11] investigated the osteogenesis and angiogenesis of ZrTiCuAl MG in SBF environments and found that both properties were superior to those of pure Ti. In addition, the oxide film on the surface of the MG formed a protective barrier, which improved the corrosion resistance. Notably, the MG not only exhibited good osteointegration, but also enhanced angiogenesis [103] as a result of the release of Cu ions. Liu et al. [104] fabricated Ni-free, Ag-containing Zr-based MGs with complex geometries and porous structures using an SLM technique. The glasses

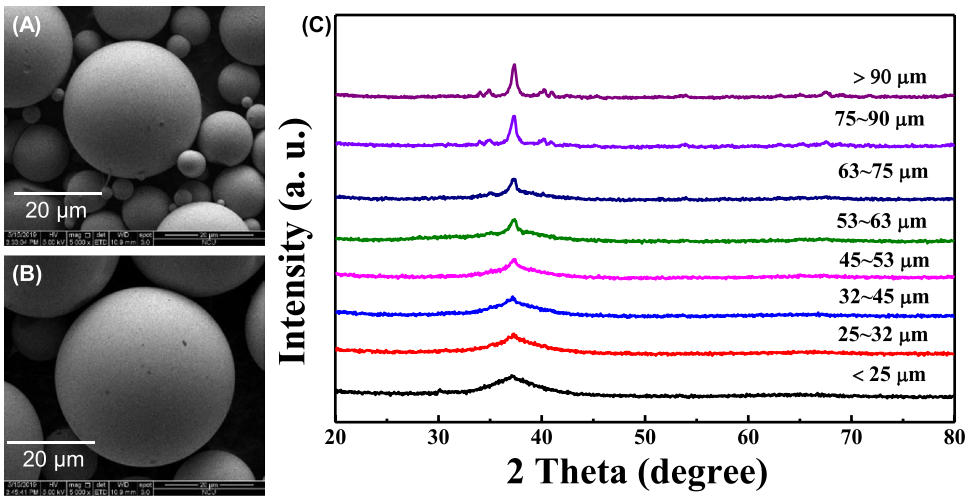

Fig. 5 The SEM images of TiZrTaSiSnCo MG powder produced by gas atomization of different sizes **a** 25- 37 µm **b** 37–44 µm and **C** the XRD patterns for the atomized powders of different sizes

were shown to possess many favorable properties, including a high degree of amorphous phase (~95%), a high density (99.7%), a high strength (> 1700 MPa), a low Young's modulus (~ 80 GPa), and a reasonable fracture toughness (36 MPa). Moreover, the glasses also exhibited excellent bio-corrosion resistance in SBF, with a released metal ion concentration after 30 days of immersion well below the safe limit for bio-implantation applications. The in vitro cell culture performance of the glasses was also comparable to that of commercial medical Ti6Al4V alloys. The porosity of the glasses was found to reach as much as 70%, with a Young's modulus of just 13 GPa and a strength of 350 MPa. Hence, the properties were comparable to those of human bone tissue [105].

3.2 Ti-Based Metallic Glass

With high strength, low weight, and excellent biocompatibility, pure Ti and its alloys (e.g., Ti6Al4V) are among the most commonly used commercial biomaterials [106]. The oxide layer formed on the surface of Ti-based materials provides good wear resistance and corrosion resistance, and hence Ti-based MG has attracted great attention for the fabrication of bio-implants [14, 107]. However, the melting point of Ti-based MG is extremely high, and therefore the manufacturing process is challenging when using traditional methods [47, 83]. Calin et al. [15] fabricated a completely amorphous structure of TiNbZrSi MGs with an amorphous structure and no harmful additions (e.g., Cu or Ni) using a casting process. The experimental results showed that the prepared materials had better corrosion resistance than commercial Ti6Al4V, with no pitting following electrochemical testing in Ringer's solution. Pang et al. [38] developed TiCuZrFeSnSiAg MG rods with a critical diameter of 7 mm using a Cu mold casting process. It was shown that the corrosion resistance and biocompatibility of the glass alloy were both better than those of the Ti6Al4V alloy.

Many studies have conducted the implantation testing of Ti-based BMGs. For example, Wang et al. [16] conducted animal experiments using the TiZrHfCuNiSiSn BMG developed by Huang et al. [96] and found that the glass bound spontaneously with bone tissue and showed both high hardness and good wear resistance. Kokubun et al. [17] enhanced the GFA of the TiZrCuPd MG developed by Zhu et al. [18] by adding 2–4% Sn. Subsequent in vivo implantation tests showed that the bone adhesion and osteointegration ability of the resulting glassy alloy were comparable to those of Ti6Al4V. Furthermore, no significant diffusion of ions was detected three months after implantation.

Huang et al. [19], investigated the electrochemical activity and biocompatibility of two TiZrSi MG systems with low (or no) toxic metal elements. The two glasses showed no significant toxicity in MTT cell assays and exhibited low inflammation and a good osteoinductive response following implantation for one month. Liao et al. [44] and Nguyen et al. [20] mixed Ti-based ground MG powder with NaCl and produced BMGs with a porous structure using a hot pressing technique. It was shown that the BMGs retained the original amorphous state of the Ti-based MG powder and had a Young's modulus of just 8 GPa. Furthermore, in vivo implantation tests showed that the sintered BMGs exhibited a good osteointegration effect after six-month in vivo tests in New Zealand white rabbits. Nguyen et al. [20] used trace amounts of Sn and Co to reduce the melting point and increase the GFA of a TiZrTaSi system. Powder material was produced by gas atomization and then hot-pressed with Al particles. The resulting powder particles had a high roundness and a completely amorphous state. Furthermore, the produced BMG had a porosity of up to 72% given the optimal addition of Al particles.

Figure 6 presents the in-vivo investigation into the feasibility of Ti-based BMG for bio-implant applications using the process shown in Fig. 3. A CT image was first acquired of the spine of a Lanyu pig with spinal injury. A plastic replica of the spine was produced using a 3D modeling and printing approach. Using the plastic replica as a model, a bone implant fabricated of Ti-based glassy alloy was created using a powder bed fusion (PBF) technique. Figure 6A shows the photo image of the pig on the next day after the implantation surgery. The pig was able to stand, indicating successful surgery for cage implantation. The pig was sacrificed 30 days after the implantation and the spine was removed for further X-ray and histology inspections. The X-ray images indicated that the implanted 3D-printed species had a good integration with the surrounding bones, as shown in Fig. 6B (frontal view) and 6C (lateral view). The removed spine was also cut and stained to determine the new in-growth tissue. The results showed that the holes of the implanted 3D-printed porous structure were occupied with newly grown tissues and the purple stain indicated that the tissues were bone cells. The results confirmed that the 3D printed prosthesis provided excellent osteointegration which may drastically reduce the stress shielding effect and prolong the lifetime of the implanted prosthesis.

3.3 Fe-Based Metallic Glass

Iron is an essential element in the human body and plays an important role in the transport, storage, and activation of molecular oxygen, together with many other important functions [22]. Stainless steel was the first alloy to be successfully used as a biological implant [107]. However, many other biodegradable Fe-based alloys have been subsequently developed. Notably, these materials not only have a degradation rate far lower than that of Mg-based materials, but also produce no hydrogen as they degrade. Thus, Fe-based MG

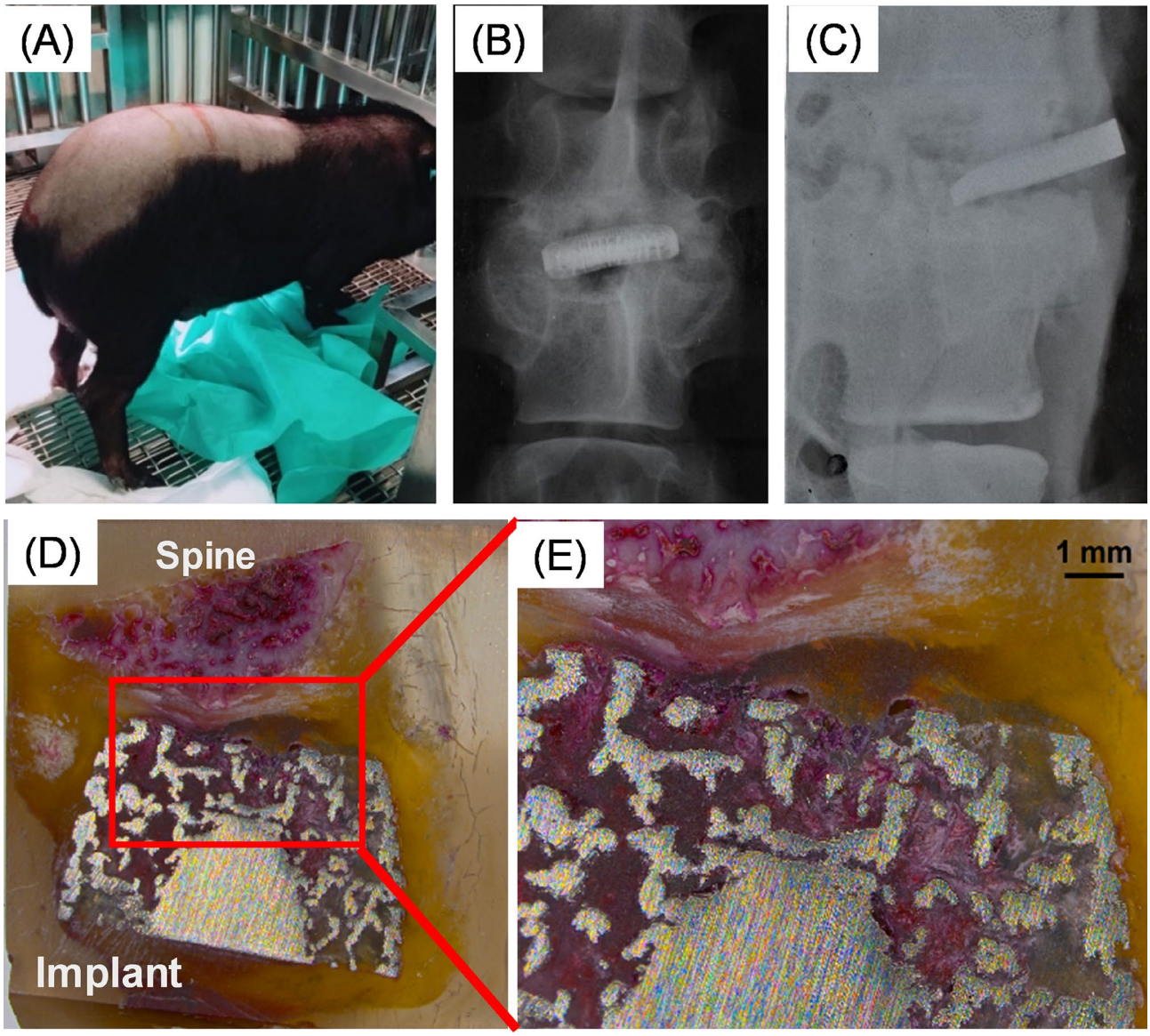

Fig. 6 In vivo test using a 18 M-old Lanyu pig **A** One day after the implant surgery, **B** front view and **C** lateral view for the X-ray images of the implant after one month **D** Cross-section histology view of the retrieved spine cage **E** Enlarged view of red box

has significant potential as an implant material. Hua et al. [23] investigated the wear behavior and corrosion resistance of FeCoCrMoCBY BMG and showed that it outperformed 316L stainless steel and CoCrMo alloy in both regards. Li et al. [21] showed that FeCrMoPC MG had better corrosion resistance in artificial saliva than Ti6Al4V and was thus a favorable candidate for dentistry applications. In addition, the results obtained in NIH3T3 cell culture tests showed that it had lower cytotoxicity and better cell adhesion performance than either 316L stainless steel or Ti6Al4V. The results of Liu et al. [108] found that FeMoPC MG had no obvious ability to inhibit Escherichia coli bacteria, but suppressed the growth of Staphylococcus aureus. Furthermore, it showed a degradation behavior similar to that of pure Fe in SBF.

Additive manufacturing (AM) enables the production of BMG without size limitations. However, Fe-based MG has high brittleness, and hence the large thermal stress produced during SLM processing readily induces microcracks. Finite element simulations were adopted to investigate the origin of these microcracks and subsequently added high-toughness Cu or CuNi alloy was added as a secondary phase to the system to form bulk metallic glass composites (BMGCs) [108, 109]. The 3D printed Fe-based BMG is fragile, with a

strength of about 106 MPa and a fracture toughness of only 2.2 MPa $m^{1/2}$. With the addition of 50 wt% Cu or CuNi, the fracture toughness of BMGCs is as high as 47 MPa $m^{1/2}$, which is about 21.4 times that of the original Fe-based BMG [110].

3.4 Mg-Based Metallic Glass

Magnesium and its divalent ions play an important role in osteogenesis, bone healing, and bone properties [111, 112]. Moreover, Mg-based biomaterials are biodegradable. After biodegradation, the implant space is replaced by new bone to form a complete biological structure, leaving no metal with corrosion and material fatigue. However, Mg-based materials prompt the evolution of hydrogen during the degradation process, which has adverse effects on the human body. Thus, while Mg-based MGs are promising candidates for biodegradable implants, their properties must be carefully controlled through the addition of appropriate elements. One of the first Mg-based MGs was the Mg-Cu-Y system developed by Inoue et al. [24, 113]. Baulin et al. [40] improved the GFA and thermal stability of the MgCaAu glassy alloy system through the addition of Yb. The results indicated that Yb was beneficial in mitigating the deleterious effects of impurities during processing.

Zberg et al. [25] studied the hydrogen evolution phenomenon of magnesium in vivo and found that Zn-rich, Mg-based MGs (about 35 at%) exhibited significantly lower hydrogen evolution than a crystalline Mg alloy reference (WZ21). Nielson [114] reviewed the biological role of strontium, an alkaline earth metal with chemical and biological properties similar to those of calcium. In general, the findings showed that, when used as an implant material, strontium tends to reduce bone resorption and promote the uptake of calcium into the bone. Li et al. [26] found that the incorporation of a small amount of strontium (~ 1 at%) into the MgZnCa system significantly improved its GFA, fracture strength and specific strength. Notably, the rapid dissolution of strontium also facilitated the formation of a surface passivation layer during the etching process, which was beneficial in controlling the degradation behavior of the material. The same group later investigated the bone-forming response of MC3T3-E1 preosteoblasts on Mg-based substrates [115]. The results showed that MgZnCaSr BMG not only had better corrosion characteristics and degradation behavior than commercial AZ31B magnesium alloy, but also prompted faster cell adhesion and diffusion in in vitro tests. Wang et al. explored the feasibility of AM techniques for the fabrication of implants using MgNdZnZr alloy [45, 116]. It was shown that the Mg-based alloy scaffolds had a porous structure with good mechanical properties and degradation behavior, and a cell activity suitable for cell adhesion and proliferation. However, several drawbacks of AM technology for the processing of Mg-based materials have been identified, including the risk of explosion and the low evaporation temperature and high vapor pressure, which promote powder splashing and lead to reduced stability of the AM process. Furthermore, AM-processed Mg-based materials are also prone to stress-corrosion cracking, such that passivation coverage is usually used to increase the durability of Mg-based alloy [117].

4 3D-Printed HEA Biomaterials

Existing HEAs can be broadly divided into two categories: HEA systems composed of Al and Fe, Co, Ni, Cr, and other elements, and refractory high-entropy alloys (RHEAs) systems composed of Ti, Ta, Nb, Zr, Hf, and so on. Since RHEAs are composed of almost exclusively of biocompatible elements, they have attracted significant interest in biomedical applications, particularly those RHEAs composed of TiTaNbZr with additional elements such as Mo or Hf to change their properties [54]. Liu et al. [59] sputtered a high-entropy alloy coating of FeCoNiAlTi on Ti6Al4V, which effectively reduced the friction coefficient of Ti6Al4V and reduced the wear that often occurs as a joint. Aksoy et al. [57, 58] sputtered equimolar TiTaNbZrHf on a NiTi shape memory alloy (SMA) substrate with a magnetron sputtering system. The RHEAs coating was found to result in a significant improvement in the mechanical strength of the substrate. Moreover, the mechanical properties of the two materials were very similar, thereby prolonging the life of the coating on the substrate during long-term mechanical loading. Finally, in immersion tests in artificial saliva and gastric juice, the released Ni ion concentration was lower than the critical value of 9 ppm required to safeguard human health [118]. Canadinc et al. [56] found that sputtered equimolar TiTaNbZrHf improved both the hardness and the Young's modulus of Ti6Al4V substrates, thereby increasing their wear resistance and suitability for long-term orthopedic implants.

Wang et al. [28] studied a novel RHEAs, TiZrHfNbFe. The research results show that RHEAs have good comprehensive mechanical properties, and also has better corrosion resistance and wear resistance than Ti_6Al_4V in the PBS solution. Motallebzadeh et al. [41] prepared TiZrTaHfNb ingots using an arc melting method and compared their wear resistance, wettability, and pitting corrosion with those of several other common biomaterials (316L stainless steel, CoCrMo and Ti6Al4V). The results showed that the prepared RHEA outperformed the other alloys in all regards. Furthermore, the presence of a high concentration of electronegative elements such as Ti and Zr in the RHEA resulted in the formation of a corrosion-resistant passivation film on the alloy surface, which improved its oxidation and corrosion resistance.

Yang et al. [42] examined the corrosion behavior and in vitro biocompatibility of TiZrHfNbTa and found that it resulted in a better adhesion, viability, and proliferation of MC3T3-E1 cells than a conventional Ti6Al4V substrate. The results indicated that the TiZr-based HEA exhibited good biocompatibility compared to that of typical Ti6Al4V alloy. Alternatively, a 900 HV of CoCrFeNiMo HEA layer was successfully formed on Ti6Al4V sheet via laser cladding technology to enhance the mechanical and chemical properties [43]. Wu et al. [61] also showed that TiTaNbZrHf exhibited no cytotoxicity toward human gingival fibroblasts (HGFs) and selectively enhanced their proliferation and adhesion rather than favoring fibrinolysis or pro-inflammatory conditions.

Hua et al. [29] studied the mechanical properties and corrosion behavior of TiZrNbTaMo systems with two different composition ratios. Similarly, Li et al. [30] also investigated the biocompatibility of TiTaNbZrMo alloy with different Ti contents. In addition, Nagase et al. [119] designed two RHEAs, TiZHfCoCrMo and TiNbTaZrMo, based on the TiZrNTMo and CoCrMo alloy system. Both RHEAs have been reported to exhibit excellent biocompatibility with pure Ti and have higher hardness. In general, the two studies confirmed that both alloy systems had excellent mechanical properties and a strong potential for biological applications. Ishimoto et al. [120] prepared TiNbTaZrMo with low porosity using a SLM technique. The test results obtained for osteoblast cultures showed that the alloy prompted the growth of osteoblasts with a broader morphology and denser network of actin fibers than those cultured on pure Ti or 316L substrates, also shown in Table 1.

Various intermetallic phases may precipitate during the conventional metallurgy process, resulting in complex HEA microstructures. Therefore, the mechanical and chemical properties of the produced HEAs are difficult to control and cracks may occur in some cases. Alternatively, the high cooling rate in the AM process prevents HEAs from precipitation and limits the formation of intermetallic phases, such that the properties of AM-produced HEAs are more controllable. Although the production of HEAs powders for AM process is still new and challenging, more researchers have joined this new field to speed up the development of 3D printed HEAs biomaterials.

5 Conclusion

This paper has presented a comprehensive review of the literature relating to the application of metallic glass (MG) and high-entropy alloys (HEAs) systems to the fabrication of biomedical implants using additive manufacturing (AM) techniques. In terms of the MG alloys, the review has focused principally on Zr-based, Ti-based, Fe-based, and Mg-based systems. By contrast, for the HEAs systems, the review has concentrated mainly on TiTaNbZr-based systems. Ti-based metallic glass is still relatively mature and has development potential. Mg-based metallic glasses also mitigate the hydrogen evolution problem that occurs when Mg alloys degrade in vivo. HEAs are still in the stage of technological development, and most of them are currently using film-forming to explore the basic properties of their materials. The review has additionally confirmed the utility of AM techniques for fabricating biomedical components with good porosity, high-precision, low Young's modulus, low cytotoxicity and high biocompatibility utilizing MG or HEAs systems. As of today, there are still a number of challenges for introducing these new intermetallic compounds to practical clinical usage, such as these materials are categorized as new materials and need to be approved as FDA Class III medical devices. The great potential for future clinical implantation is still attractive for researchers who are working in this field by combining the AM process and newly developed IMCs. Overall, the findings of this review suggest that the combination of metal glass alloys and AM technology will continue to generate many fruitful research and development opportunities for biological implants and related applications for years to come.

References

1. Gepreel, M. A. H., & Niinomi, M. (2013). Biocompatibility of Ti-alloys for long-term implantation. *Journal of the Mechanical Behavior of Biomedical Materials, 20*, 407–415.
2. Merritt, K., & Brown, S. A. (1988). Effect of proteins and pH on fretting corrosion and metal ion release. *Journal of Biomedical Materials Research, 22*(2), 111–120.
3. Williams, R. L., Brown, S. A., & Merritt, K. (1988). Electrochemical studies on the influence of proteins on the corrosion of implant alloys. *Biomaterials, 9*(2), 181–186.
4. Granchi, D., Cenni, E., Ciapetti, G., Savarino, L., Stea, S., Gamberini, S., Gori, A., & Pizzoferrato, A. (1998). Cell death induced by metal ions: necrosis or apoptosis? *Journal of Materials Science: Materials in Medicine, 9*(1), 31–37.
5. Hanawa, T. (2004). Metal ion release from metal implants. *Materials Science and Engineering: C, 24*(6–8), 745–752.
6. Daguano, J. K. M. B., Giora, F. C., Santos, K. F., Pereira, A. B. G. C., Souza, M. T., Davila, J. L., Rodas, A. C. D., & Santos,

C. (2022). Shear-thinning sacrificial ink for fabrication of Biosilicate (R) osteoconductive scaffolds by material extrusion 3D printing. *Materials Chemistry and Physics*. https://doi.org/10.1016/j.matchemphys.2022.126286
7. Gul, H., Khan, M., & Khan, A. S. (2020) Bioceramics: Types and clinical applications, *Handbook of Ionic Substituted Hydroxyapatites,* Elsevier 53–83.
8. Sadasivuni, K. K., Saha, P., Adhikari, J., Deshmukh, K., Ahamed, M. B., & Cabibihan, J. J. (2020). Recent advances in mechanical properties of biopolymer composites: A review. *Polymer Composites, 41*(1), 32–59.
9. Virtanen, S. (2011). Biodegradable Mg and Mg alloys: Corrosion and biocompatibility. *Materials Science and Engineering: B, 176*(20), 1600–1608.
10. Kim, M., An, S., Huh, C., & Kim, C. (2019). Development of zirconium-based alloys with low elastic modulus for dental implant materials. *Applied Sciences, 9*(24), 5281.
11. Sun, K., Fu, R., Liu, X., Xu, L., Wang, G., Chen, S., Zhai, Q., & Pauly, S. (2022). Osteogenesis and angiogenesis of a bulk metallic glass for biomedical implants. *Bioactive Materials, 8*, 253–266.
12. Chen, Q., Liu, L., & Zhang, S. M. (2010). The potential of Zr-based bulk metallic glasses as biomaterials. *Frontiers of Materials Science in China, 4*(1), 34–44.
13. Sun, Y., Huang, Y., Fan, H., Liu, F., Shen, J., Sun, J., & Chen, J. J. J. (2014). Comparison of mechanical behaviors of several bulk metallic glasses for biomedical application. *Journal of Non-Crystalline Solids, 406*, 144–150.
14. Gong, P., Deng, L., Jin, J., Wang, S., Wang, X., & Yao, K. (2016). Review on the research and development of Ti-based bulk metallic glasses. *Metals, 6*(11), 264.
15. Calin, M., Gebert, A., Ghinea, A. C., Gostin, P. F., Abdi, S., Mickel, C., & Eckert, J. (2013). Designing biocompatible Ti-based metallic glasses for implant applications. *Materials Science and Engineering: C, 33*(2), 875–883.
16. Wang, Y., Li, H., Cheng, Y., Zheng, Y., & Ruan, L. (2013). In vitro and in vivo studies on Ti-based bulk metallic glass as potential dental implant material. *Materials Science and Engineering: C, 33*(6), 3489–3497.
17. Kokubun, R., Wang, W., Zhu, S., Xie, G., Ichinose, S., Itoh, S., & Takakuda, K. (2015). In vivo evaluation of a Ti-based bulk metallic glass alloy bar. *Bio-medical Materials and Engineering, 26*(1–2), 9–17.
18. Zhu, S., Xie, G., Qin, F., Wang, X., & Inoue, A. (2012). Effect of minor Sn additions on the formation and properties of TiCuZrPd bulk glassy alloy. *Materials Transactions*. https://doi.org/10.2320/matertrans.M2011281
19. Huang, C., Huang, Y., Lin, Y., Lin, C., Huang, J., Chen, C., Li, J., Chen, Y., & Jang, J. (2014). Electrochemical and biocompatibility response of newly developed TiZr-based metallic glasses. *Materials Science and Engineering: C, 43*, 343–349.
20. Nguyen, V. T., Wong, X. P. C., Song, S.-M., Tsai, P. H., Jang, J. S. C., Tsao, I. Y., Lin, C. H., & Nguyen, V. C. (2020). Open-cell tizr-based bulk metallic glass scaffolds with excellent biocompatibility and suitable mechanical properties for biomedical application. *Journal of functional biomaterials, 11*(2), 28.
21. Li, S., Wei, Q., Li, Q., Jiang, B., Chen, Y., & Sun, Y. (2015). Development of Fe-based bulk metallic glasses as potential biomaterials. *Materials Science and Engineering: C, 52*, 235–241.
22. Gorejová, R., Haverová, L., Oriňaková, R., Oriňak, A., & Oriňak, M. (2019). Recent advancements in Fe-based biodegradable materials for bone repair. *Journal of Materials Science, 54*(3), 1913–1947.
23. Hua, N., Hong, X., Liao, Z., Zhang, L., Ye, X., Wang, Q., & Liaw, P. K. (2020). Corrosive wear behaviors and mechanisms of a biocompatible Fe-based bulk metallic glass. *Journal of Non-Crystalline Solids, 542*, 120088.
24. Inoue, A., Kato, A., Zhang, T., Kim, S., Masumoto, T. M., & Mg-Cu, Y. (1991). Mg-Cu–Y amorphous alloys with high mechanical strengths produced by a metallic mold casting method. *Materials Transactions JIM, 32*, 609–616.
25. Zberg, B., Uggowitzer, P. J., & Löffler, J. F. (2009). MgZnCa glasses without clinically observable hydrogen evolution for biodegradable implants. *Nature materials, 8*(11), 887–891.
26. Li, H., Pang, S., Liu, Y., Sun, L., Liaw, P. K., & Zhang, T. (2015). Biodegradable Mg–Zn–Ca–Sr bulk metallic glasses with enhanced corrosion performance for biomedical applications. *Materials & Design, 67*, 9–19.
27. Shaw, D. (2012). *Atomic diffusion in semiconductors*. Springer Science & Business Media.
28. Wang, W., Yang, K., Wang, Q., Dai, P., Fang, H., Wu, F., Guo, Q., Liaw, P. K., & Hua, N. (2022). Novel Ti-Zr-Hf-Nb-Fe refractory high-entropy alloys for potential biomedical applications. *Journal of Alloys and Compounds, 906*, 164383.
29. Hua, N., Wang, W., Wang, Q., Ye, Y., Lin, S., Zhang, L., Guo, Q., Brechtl, J., & Liaw, P. K. (2021). Mechanical, corrosion, and wear properties of biomedical Ti–Zr–Nb–Ta–Mo high entropy alloys. *Journal of Alloys and Compounds, 861*, 157997.
30. Li, C., Ma, Y., Yang, X., & Hou, M. (2021). New TiTaNbZrMo high-entropy alloys for metallic biomaterials. *Materials Research Express, 8*(10), 105403.
31. Morrison, M. L., Buchanan, R. A., Leon, R. V., Liu, C. T., Green, B. A., Liaw, P. K., & Horton, J. A. (2005). The electrochemical evaluation of a Zr-based bulk metallic glass in a phosphate-buffered saline electrolyte. *Journal of Biomedical Materials Research. Part A, 74*(3), 430–438.
32. Giesen, E., Ding, M., Dalstra, M., & Van Eijden, T. (2001). Mechanical properties of cancellous bone in the human mandibular condyle are anisotropic. *Journal of biomechanics, 34*(6), 799–803.
33. Niinomi, M. (1998). Mechanical properties of biomedical titanium alloys. *Materials Science and Engineering: A, 243*(1–2), 231–236.
34. Takeuchi, A., & Inoue, A. (2001). Quantitative evaluation of critical cooling rate for metallic glasses. *Materials Science and Engineering: A, 304*, 446–451.
35. Halim, Q., Mohamed, N. A. N., Rejab, M. R. M., Naim, W. N. W. A., & Ma, Q. (2021). Metallic glass properties, processing method and development perspective: a review. *The International Journal of Advanced Manufacturing Technology, 112*(5), 1231–1258.
36. Basu, J., & Ranganathan, S. (2003). Bulk metallic glasses: A new class of engineering materials. *Sadhana, 28*(3–4), 783–798.
37. Raja, V., & Ranganathan, S. (1988). Effect of molybdenum and silicon on the electrochemical corrosion behavior of fenib metallic glasses. *Corrosion, 44*(5), 263–270.
38. Pang, S., Liu, Y., Li, H., Sun, L., Li, Y., & Zhang, T. (2015). New Ti-based Ti–Cu–Zr–Fe–Sn–Si–Ag bulk metallic glass for biomedical applications. *Journal of Alloys and Compounds, 625*, 323–327.
39. Liu, Y., Wang, Y. M., Pang, H. F., Zhao, Q., & Liu, L. (2013). A Ni-free ZrCuFeAlAg bulk metallic glass with potential for biomedical applications. *Acta Biomaterialia, 9*(6), 7043–7053.
40. Baulin, O., Fabregue, D., Kato, H., Liens, A., Wada, T., & Pelletier, J. M. (2018). A new, toxic element-free Mg-based metallic glass for biomedical applications. *Journal of Non-Crystalline Solids, 481*, 397–402.
41. Motallebzadeh, A., Peighambardoust, N. S., Sheikh, S., Murakami, H., Guo, S., & Canadinc, D. (2019). Microstructural, mechanical and electrochemical characterization of TiZrTaHfNb

and Ti1. 5ZrTa0. 5Hf0. 5Nb0.5 refractory high-entropy alloys for biomedical applications. *Intermetallics, 113*, 106572.
42. Yang, W., Liu, Y., Pang, S., Liaw, P. K., & Zhang, T. (2020). Biocorrosion behavior and in vitro biocompatibility of equimolar TiZrHfNbTa high-entropy alloy. *Intermetallics, 124*, 106845.
43. Deng, C., Wang, C., Chai, L., Wang, T., & Luo, J. (2022). Mechanical and chemical properties of CoCrFeNiMo0.2 high entropy alloy coating fabricated on Ti6Al4V by laser cladding. *Intermetallics, 144*, 107504.
44. Liao, Y., Song, S., Li, T., Li, J., Tsai, P., Jang, J., Huang, C., Huang, J., Huang, Y., & Lin, C. (2020). Synthesis and characterization of an open-pore toxic-element-free Ti-based bulk metallic glass foam for bio-implant application. *Journal of Materials Research and Technology, 9*(3), 4518–4526.
45. Wang, Y., Fu, P., Wang, N., Peng, L., Kang, B., Zeng, H., Yuan, G., & Ding, W. (2020). Challenges and solutions for the additive manufacturing of biodegradable magnesium implants. *Engineering, 6*(11), 1267–1275.
46. Klement, W., Willens, R., & Duwez, P. (1960). Non-crystalline structure in solidified gold–silicon alloys. *Nature, 187*(4740), 869–870.
47. Meagher, P., O'Cearbhaill, E. D., Byrne, J. H., & Browne, D. J. (2016). Bulk metallic glasses for implantable medical devices and surgical tools. *Advanced Materials, 28*(27), 5755–5762.
48. Schroers, J., Kumar, G., Hodges, T. M., Chan, S., & Kyriakides, T. R. (2009). Bulk metallic glasses for biomedical applications. *JOM Journal of the Minerals Metals and Materials Society, 61*(9), 21–29.
49. Chen, H. (1980). Glassy metals. *Reports on Progress in Physics, 43*(4), 353.
50. Chen, M. (2011). A brief overview of bulk metallic glasses. *NPG Asia Materials, 3*(9), 82–90.
51. Pauly, S., Wang, P., Kühn, U., & Kosiba, K. (2018). Experimental determination of cooling rates in selectively laser-melted eutectic Al-33Cu. *Additive Manufacturing, 22*, 753–757.
52. Jien Wei, Y. (2006). Recent progress in high entropy alloys. *Annals de Chimie Science de Materiaux, 31*(6), 633–648.
53. Miracle, D. B., & Senkov, O. N. (2017). A critical review of high entropy alloys and related concepts. *Acta Materialia, 122*, 448–511.
54. Castro, D., Jaeger, P., Baptista, A. C., & Oliveira, J. P. (2021). An overview of high-entropy alloys as biomaterials. *Metals, 11*(4), 648.
55. Li, W., Liu, P., & Liaw, P. K. (2018). Microstructures and properties of high-entropy alloy films and coatings: A review. *Materials Research Letters, 6*(4), 199–229.
56. Tüten, N., Canadinc, D., Motallebzadeh, A., & Bal, B. (2019). Microstructure and tribological properties of TiTaHfNbZr high entropy alloy coatings deposited on Ti6Al4V substrates. *Intermetallics, 105*, 99–106.
57. Motallebzadeh, A., Yagci, M., Bedir, E., Aksoy, C., & Canadinc, D. (2018). Mechanical properties of TiTaHfNbZr high-entropy alloy coatings deposited on NiTi shape memory alloy substrates. *Metallurgical and Materials Transactions A, 49*(6), 1992–1997.
58. Aksoy, C., Canadinc, D., & Yagci, M. (2019). Assessment of Ni ion release from TiTaHfNbZr high entropy alloy coated NiTi shape memory substrates in artificial saliva and gastric fluid. *Materials Chemistry and Physics, 236*, 121802.
59. Liu, D., Ma, Z., Zhang, W., Huang, B., Zhao, H., & Ren, L. (2021). Superior antiwear biomimetic artificial joint based on high-entropy alloy coating on porous Ti6Al4V. *Tribology International, 158*, 106937.
60. Wang, S. P., & Xu, J. (2017). TiZrNbTaMo high-entropy alloy designed for orthopedic implants: As-cast microstructure and mechanical properties. *Materials Science and Engineering: C, 73*, 80–89.
61. Wang, S., Wu, D., She, H., Wu, M., Shu, D., Dong, A., Lai, H., & Sun, B. (2020). Design of high-ductile medium entropy alloys for dental implants. *Materials Science and Engineering: C, 113*, 110959.
62. Yeh, J. W., Chen, S. K., Lin, S. J., Gan, J. Y., Chin, T. S., Shun, T. T., Tsau, C. H., & Chang, S. Y. (2004). Nanostructured high-entropy alloys with multiple principal elements: Novel alloy design concepts and outcomes. *Advanced Engineering Materials, 6*(5), 299–303.
63. Jien Wei, Y. (2013). Alloy design strategies and future trends in high-entropy alloys. *JOM Journal of the Minerals Metals and Materials Society, 65*(12), 1759–1771.
64. Guo, S., Ng, C., Lu, J., & Liu, C. (2011). Effect of valence electron concentration on stability of fcc or bcc phase in high entropy alloys. *Journal of Applied Physics, 109*(10), 103505.
65. Chen, J., Zhou, X., Wang, W., Liu, B., Lv, Y., Yang, W., Xu, D., & Liu, Y. (2018). A review on fundamental of high entropy alloys with promising high–temperature properties. *Journal of Alloys and Compounds, 760*, 15–30.
66. Tsai, K. Y., Tsai, M. H., & Yeh, J. W. (2013). Sluggish diffusion in Co–Cr–Fe–Mn–Ni high-entropy alloys. *Acta Materialia, 61*(13), 4887–4897.
67. Temkin, D. E. (1972). One-dimensional random walks in a two-component chain. *Soviet Math Docl, 13*, 1172–1176.
68. Senkov, O. N., Wilks, G., Scott, J., & Miracle, D. B. (2011). Mechanical properties of Nb25Mo25Ta25W25 and V20Nb-20Mo20Ta20W20 refractory high entropy alloys. *Intermetallics, 19*(5), 698–706.
69. Kao, Y. F., Chen, S. K., Chen, T. J., Chu, P. C., Yeh, J. W., & Lin, S. J. (2011). Electrical, magnetic, and Hall properties of AlxCo-CrFeNi high-entropy alloys. *Journal of Alloys and Compounds, 509*(5), 1607–1614.
70. Lu, C. L., Lu, S. Y., Yeh, J. W., & Hsu, W. K. (2013). Thermal expansion and enhanced heat transfer in high-entropy alloys. *Journal of Applied Crystallography, 46*(3), 736–739.
71. Yeh, J. W., Chang, S. Y., Hong, Y. D., Chen, S. K., & Lin, S. J. (2007). Anomalous decrease in X-ray diffraction intensities of Cu–Ni–Al–Co–Cr–Fe–Si alloy systems with multi-principal elements. *Materials Chemistry and Physics, 103*(1), 41–46.
72. Ranganathan, S. (2003). Alloyed pleasures: Multimetallic cocktails. *Current Science, 85*(10), 1404–1406.
73. Xian, X., Zhong, Z. H., Lin, L. J., Zhu, Z. X., Chen, C., & Wu, Y. C. (2018). Tailoring strength and ductility of high-entropy CrMnFeCoNi alloy by adding Al. *Rare Metals*. https://doi.org/10.1007/s12598-018-1161-4
74. Li, C., Li, J., Zhao, M., & Jiang, Q. (2009). Effect of alloying elements on microstructure and properties of multiprincipal elements high-entropy alloys. *Journal of Alloys and Compounds, 475*(1–2), 752–757.
75. Ngo, T. D., Kashani, A., Imbalzano, G., Nguyen, K. T., & Hui, D. (2018). Additive manufacturing (3D printing): A review of materials, methods, applications and challenges. *Composites Part B: Engineering, 143*, 172–196.
76. Melchels, F. P., Feijen, J., & Grijpma, D. W. (2010). A review on stereolithography and its applications in biomedical engineering. *Biomaterials, 31*(24), 6121–6130.
77. Popescu, D., Zapciu, A., Amza, C., Baciu, F., & Marinescu, R. (2018). FDM process parameters influence over the mechanical properties of polymer specimens: A review. *Polymer Testing, 69*, 157–166.
78. Sing, S. L., Yeong, W. Y., Wiria, F. E., Tay, B. Y., Zhao, Z., Zhao, L., Tian, Z., & Yang, S. (2017). Direct selective laser sintering

and melting of ceramics: a review. *Rapid Prototyping Journal*. https://doi.org/10.1108/RPJ-11-2015-0178
79. Yap, C. Y., Chua, C. K., Dong, Z. L., Liu, Z. H., Zhang, D. Q., Loh, L. E., & Sing, S. L. (2015). Review of selective laser melting: Materials and applications. *Applied Physics Reviews, 2*(4), 041101.
80. Liu, M., Kumar, A., Bukkapatnam, S., & Kuttolamadom, M. (2021). A Review of the anomalies in directed energy deposition (DED) processes & potential solutions-part quality & defects. *Procedia Manufacturing, 53*, 507–518.
81. Pauly, S., Löber, L., Petters, R., Stoica, M., Scudino, S., Kühn, U., & Eckert, J. (2013). Processing metallic glasses by selective laser melting. *Materials Today, 16*(1–2), 37–41.
82. Tang, M., Pistorius, P. C., Narra, S., & Beuth, J. L. (2016). Rapid solidification: Selective laser melting of AlSi10Mg. *JOM Journal of the Minerals Metals and Materials Society, 68*(3), 960–966.
83. Deng, L., Wang, S., Wang, P., Kühn, U., & Pauly, S. (2018). Selective laser melting of a Ti-based bulk metallic glass. *Materials Letters, 212*, 346–349.
84. Liu, R., Wang, Z. T., Sparks, Liou, F., & Newkirk, J. (2017). Aerospace applications of laser additive manufacturing, *Laser additive manufacturing,* 351–371.
85. Angrish, A. (2014). A critical analysis of additive manufacturing technologies for aerospace applications. *2014 IEEE Aerospace Conference*. https://doi.org/10.1109/AERO.2014.6836456
86. Schiller, G. (2015). Additive manufacturing for Aerospace. *2015 IEEE Aerospace Conference*. https://doi.org/10.1109/AERO.2015.7118958
87. Bose, S., Ke, D., Sahasrabudhe, H., & Bandyopadhyay, A. (2018). Additive manufacturing of biomaterials. *Progress in materials science, 93*, 45–111.
88. Zadpoor, A. A., & Malda, J. (2017). Additive manufacturing of biomaterials, tissues, and organs. *Annals of Biomedical Engineering, 45*(1), 1–11.
89. Lim, S., Buswell, R. A., Le, T. T., Austin, S. A., Gibb, A. G., & Thorpe, T. (2012). Developments in construction-scale additive manufacturing processes. *Automation in construction, 21*, 262–268.
90. Bos, F., Wolfs, R., Ahmed, Z., & Salet, T. (2016). Additive manufacturing of concrete in construction: Potentials and challenges of 3D concrete printing. *Virtual and Physical Prototyping, 11*(3), 209–225.
91. Yang, F., Chen, C., Zhou, Q., Gong, Y., Li, R., Li, C., Klämpfl, F., Freund, S., Wu, X., & Sun, Y. (2017). Laser beam melting 3D printing of Ti6Al4V based porous structured dental implants: Fabrication, biocompatibility analysis and photoelastic study. *Scientific Reports, 7*(1), 1–12.
92. Li, S., Li, X., Hou, W., Nune, K. C., Misra, R. D. K., Correa-Rodriguez, V. L., Guo, Z., Hao, Y., Yang, R., & Murr, L. E. (2018). Fabrication of open-cellular (porous) titanium alloy implants: Osseointegration, vascularization and preliminary human trials. *Science China Materials, 61*(4), 525–536.
93. Habibovic, P., Yuan, H., van den Doel, M., Sees, T. M., van Blitterswijk, C. A., & de Groot, K. (2006). Relevance of osteoinductive biomaterials in critical-sized orthotopic defect. *Journal of Orthopaedic Research, 24*(5), 867–876.
94. Zindani, D., Kumar, K., & Davim, J. P. (2019) Metallic biomaterials—A review, Mechanical Behaviour of Biomaterials 83-99
95. Arabnejad, S., Johnston, B., Tanzer, M., & Pasini, D. (2017). Fully porous 3D printed titanium femoral stem to reduce stress-shielding following total hip arthroplasty. *Journal of Orthopaedic Research, 35*(8), 1774–1783.
96. Huang, Y., Shen, J., Sun, J., & Yu, X. (2007). A new Ti–Zr–Hf–Cu–Ni–Si–Sn bulk amorphous alloy with high glass-forming ability. *Journal of Alloys and Compounds, 427*(1–2), 171–175.
97. Popescu, S. M., Manolea, H. O., Diaconu, O. A., Mercuţ, R., Scrieciu, M., Dascălu, I. T., Ţuculină, M. J., Obădan, F., & Popescu, F. D. (2017). Zirconia biocompatibility in animal studies-a systematic review. *Defect and Diffusion Forum, 376*, 12–28.
98. Sun, Y. S., Zhang, W., Kai, W., Liaw, P. K., & Huang, H. H. (2014). Evaluation of Ni-free Zr–Cu–Fe–Al bulk metallic glass for biomedical implant applications. *Journal of Alloys and Compounds, 586*, S539–S543.
99. Sun, Y., Huang, Y., Fan, H., Wang, Y., Ning, Z., Liu, F., Feng, D., Jin, X., Shen, J., & Sun, J. (2015). In vitro and in vivo biocompatibility of an Ag-bearing Zr-based bulk metallic glass for potential medical use. *Journal of Non-Crystalline Solids, 419*, 82–91.
100. Yamamoto, A., Honma, R., & Sumita, M. (1998). Cytotoxicity evaluation of 43 metal salts using murine fibroblasts and osteoblastic cells. *Journal of Biomedical Materials Research: An Official Journal of The Society for Biomaterials, The Japanese Society for Biomaterials, and the Australian Society for Biomaterials, 39*(2), 331–340.
101. Chen, H. W., Hsu, K.-C., Chan, Y. C., Duh, J. G., Lee, J.-W., Jang, J. S. C., & Chen, G. J. (2014). Antimicrobial properties of Zr–Cu–Al–Ag thin film metallic glass. *Thin Solid Films, 561*, 98–101.
102. Hua, N., Huang, L., Chen, W., He, W., & Zhang, T. (2014). Biocompatible Ni-free Zr-based bulk metallic glasses with high-Zr-content: Compositional optimization for potential biomedical applications. *Materials Science and Engineering: C, 44*, 400–410.
103. Eisenbarth, E., Velten, D., Müller, M., Thull, R., & Breme, J. (2004). Biocompatibility of β-stabilizing elements of titanium alloys. *Biomaterials, 25*(26), 5705–5713.
104. Zhang, C., Li, X., Liu, S., Liu, H., Yu, L., & Liu, L. (2019). 3D printing of Zr-based bulk metallic glasses and components for potential biomedical applications. *Journal of Alloys and Compounds, 790*, 963–973.
105. Wu, D., Isaksson, P., Ferguson, S. J., & Persson, C. (2018). Young's modulus of trabecular bone at the tissue level: A review. *Acta Biomaterialia, 78*, 1–12.
106. Pandey, A., Awasthi, A., & Saxena, K. K. (2020). Metallic implants with properties and latest production techniques: A review. *Advances in Materials and Processing Technologies, 6*(2), 405–440.
107. Zaman, H. A., Sharif, S., Idris, M. H., & Kamarudin, A. (2015). Metallic biomaterials for medical implant applications: a review. *Applied Mechanics and Materials, 735*, 19–25.
108. Liu, R., He, R., Xiao, J., Tang, M., Zhang, H., & Guo, S. (2019). Development of Fe-based bulk metallic glass composite as biodegradable metal. *Materials Letters, 247*, 185–188.
109. Han, B., Zhang, C., & Shi, M. (2022). Molecular dynamics simulations of nanoindentation of CuNi alloy. *International Journal of Applied Mechanics, 14*(2), 2250011.
110. Li, N., Zhang, J., Xing, W., Ouyang, D., & Liu, L. (2018). 3D printing of Fe-based bulk metallic glass composites with combined high strength and fracture toughness. *Materials & Design, 143*, 285–296.
111. Walker, J., Shadanbaz, S., Woodfield, T. B., Staiger, M. P., & Dias, G. J. (2014). Magnesium biomaterials for orthopedic application: A review from a biological perspective. *Journal of Biomedical Materials Research Part B: Applied Biomaterials, 102*(6), 1316–1331.
112. Chaya, A., Yoshizawa, S., Verdelis, K., Myers, N., Costello, B. J., Chou, D. T., Pal, S., Maiti, S., Kumta, P. N., & Sfeir, C. (2015). In vivo study of magnesium plate and screw degradation and bone fracture healing. *Acta Biomaterialia, 18*, 262–269.
113. Bin, S. J. B., Fong, K. S., Chua, B. W., & Gupta, M. (2021). Mg-based bulk metallic glasses: A review of recent developments, *Journal of Magnesium and Alloys*.

114. Nielsen, S. P. (2004). The biological role of strontium. *Bone, 35*(3), 583–588.
115. Li, H., He, W., Pang, S., Liaw, P. K., & Zhang, T. (2016). In vitro responses of bone-forming MC3T3-E1 pre-osteoblasts to biodegradable Mg-based bulk metallic glasses. *Materials Science and Engineering: C, 6*, 632–641.
116. Qin, H., Zhao, Y., An, Z., Cheng, M., Wang, Q., Cheng, T., Wang, Q., Wang, J., Jiang, Y., & Zhang, X. (2015). Enhanced antibacterial properties, biocompatibility, and corrosion resistance of degradable Mg-Nd-Zn-Zr alloy. *Biomaterials, 53*, 211–220.
117. Scully, J. R., Gebert, A., & Payer, J. H. (2007). Corrosion and related mechanical properties of bulk metallic glasses. *Journal of Materials research, 22*(2), 302–313.
118. Alcantar, N. A., Aydil, E. S., & Israelachvili, J. N. (2000). Polyethylene glycol–coated biocompatible surfaces. *Journal of Biomedical Materials Research: An Official Journal of The Society for Biomaterials, The Japanese Society for Biomaterials, and The Australian Society for Biomaterials and the Korean Society for Biomaterials, 51*(3), 343–351.
119. Nagase, T., Iijima, Y., Matsugaki, A., Ameyama, K., & Nakano, T. (2020). Design and fabrication of Ti–Zr-Hf-Cr-Mo and Ti–Zr-Hf-Co-Cr-Mo high-entropy alloys as metallic biomaterials. *Materials Science and Engineering: C, 107*, 110322.
120. Ishimoto, T., Ozasa, R., Nakano, K., Weinmann, M., Schnitter, C., Stenzel, M., Matsugaki, A., Nagase, T., Matsuzaka, T., & Todai, M. (2021). Development of TiNbTaZrMo bio-high entropy alloy (BioHEA) super-solid solution by selective laser melting, and its improved mechanical property and biocompatibility. *Scripta Materialia, 194*, 113658.